Design Procedure for Two-Stage CMOS Operational Amplifiers Employing Current Buffer

J. Mahattanakul, *Member, IEEE*

***Abstract*—The design procedure of the two-stage CMOS operational amplifiers employing Miller capacitor in conjunction with the common-gate current buffer is presented. Unlike the previously reported design strategy of the opamp of this type, which results in the opamp with a pair of nondominant complex conjugate poles and a finite zero, the proposed procedure is based upon the design strategy that results in the opamp with only one dominant pole. Design example of the proposed procedure is given.**

***Index Terms*—CMOS analog integreated circuit, frequency compensation, operational amplifier, poles and zeros.**

I. Introduction

TO AVOID closed-loop instability, frequency compensation is necessary in opamp design [1]–[7]. For two-stage CMOS opamp, the simplest compensation technique is to connect a capacitor across the high gain stage. This results in the pole splitting phenomena which improves the closed-loop stability significantly. However, due to the feed-forward path through the Miller capacitor, a right-half-plane (RHP) zero is also created. In theory, such a zero can be nullified if the compensation capacitor is connected in conjunction with either a nullifying resistor or a common-gate current buffer (Fig. 1). The design procedures of the former type of opamp have been proposed, e.g., in [2] and more recently in [3]. However since both the procedures in [2] and [3] employ pole–zero cancellation, they are sensitive to process and temperature variation.

Although the implementation of the opamp with current buffer compensation has been reported [4] and the design strategy has been proposed [1], the complete design procedure for the opamp of this type has never been presented. In this paper, we attempt to fill the gap by proposing the design procedure for the CMOS opamp with Miller compensation in conjunction with the current buffer.

It should be pointed out that unlike the strategy proposed in [1], which results in the opamp with a pair of complex conjugate poles and one finite zero, the proposed design procedure is based on the strategy which would theoretically result in the opamp with only one real nondominant pole. The differences of the closed-loop behavior between these two compensation conditions will be considered in the next section.

Manuscript received January 4, 2004; revised March 8, 2005. This paper was recommended by Associate Editor A. Apsel.

The author is with the Electronic Engineering Department, Mahanakorn University of Technology, Bangkok 10530, Thailand (e-mail: jirayut@mut.ac.th).

Digital Object Identifier 10.1109/TCSII.2005.852530

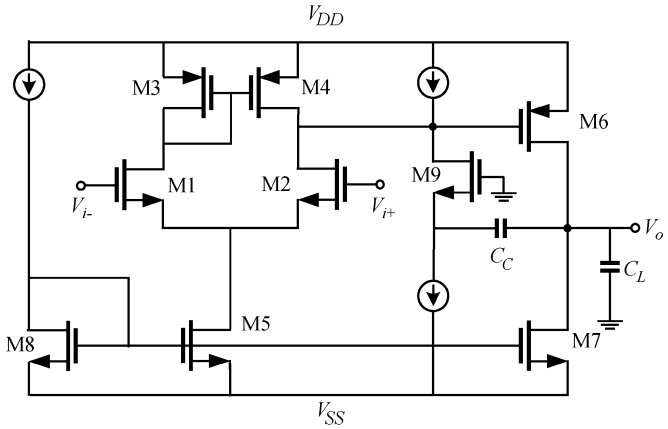

Fig. 1. Two-stage CMOS opamp with Miller capacitor and a common-gate current buffer.

II. Frequency Compensation Consideration

Generally, the transfer function of the opamp with three poles and one finite zero can be expressed as

$$A(s) = \frac{A_O\left(1-\frac{s}{z}\right)}{\left(1-\frac{s}{p_1}\right)\left(1-\frac{s}{p_2}\right)\left(1-\frac{s}{p_3}\right)}. \tag{1}$$

Referring to (1), if p_1 is real, we have

$$A(s) = \frac{A_O\left(1-\frac{s}{z}\right)}{\left(1+\frac{s}{\omega_{p_1}}\right)\left(1+\frac{2\xi s}{\omega_o}+\frac{s^2}{\omega_o^2}\right)} \tag{2}$$

where $\omega_{p1} = -p_1$ is a pole frequency associated with the real pole p_1 and ξ and ω_o are, respectively, the damping factor and the natural undamped frequency corresponding to the nondominant poles p_2 and p_3.

By denoting ω_u the unity-gain frequency and

$$\phi_M = 180^\circ - \angle A(j\omega_u) \tag{3}$$

the phase margin of the opamp, the relationship between the parameters ω_o, ω_u, ϕ_M and z can be shown to be

$$\omega_o = \frac{\omega_u a}{\xi - \sqrt{\xi^2 + a^2}} \tag{4}$$

where

$$a = \tan\left(\phi_M + \tan^{-1}\frac{-z}{\omega_u}\right).$$

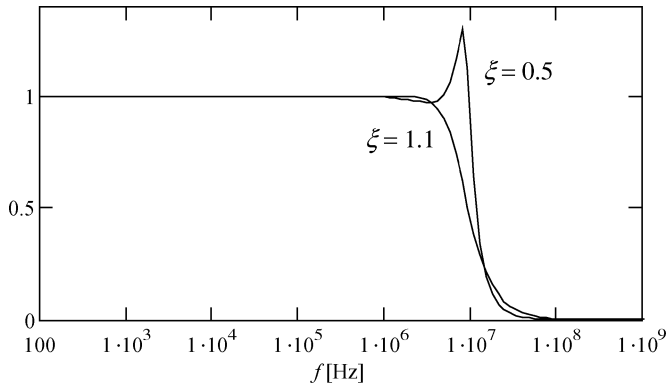

Fig. 2. Magnitude response of the opamp with $\phi_M = 63.5°$, $\omega_u = 2\pi \times 5\ \mathrm{Mrad/s}$ and $z = -5\omega_u$ connected as the voltage follower (100% feedback).

Consequently, the required phase margin can be obtained if the value of ω_o and ξ are chosen in accordance to (4). However, as depicted in Fig. 2, the closed-loop response of the opamp with feedback connection cannot be determined by the phase margin alone. The damping factor ξ of the nondominant poles also plays a critical role in shaping the closed-loop response of the opamp. According to Fig. 2, for $\xi < 1$, which is the condition that results in p_2 and p_3 becoming complex conjugate pair, the peaking in closed-loop response is evident. The compensation condition that results in complex nondominant poles should therefore be cautiously employed.

According to (1), the nondominant poles, p_2 and p_3, are real if $\xi > 1$. It was found that under such a condition, the values of p_3 and z can be made equal if the relationship

$$\omega_o = \frac{-z}{\xi + \sqrt{\xi^2 - 1}} \tag{5}$$

is satisfied.

Accordingly, by equating (4) and (5), we found that the value of ξ that results in the opamp with one nondominant pole and a specified value of phase margin is given by

$$\xi = \frac{-\left(\omega_u^2 + z^2\right) a}{2\sqrt{\omega_u z(az - \omega_u)(a\omega_u + z)}}. \tag{6}$$

For instance, by using (6) we found that for $z = -5\omega_u$, the opamp with only one nondominant pole and $\phi_M = 63.5°$ can be obtained if ξ is chosen to be about 1.1.

Furthermore, it can also be shown that if the opamp with one non dominant pole is connected as the voltage follower, the quality factor of the resulting circuit is

$$Q = \frac{1}{\sqrt{\tan \phi_M}}. \tag{7}$$

For example, the phase margin of 63.5° will gives rise to the Q of 0.707 (maximally flat response).

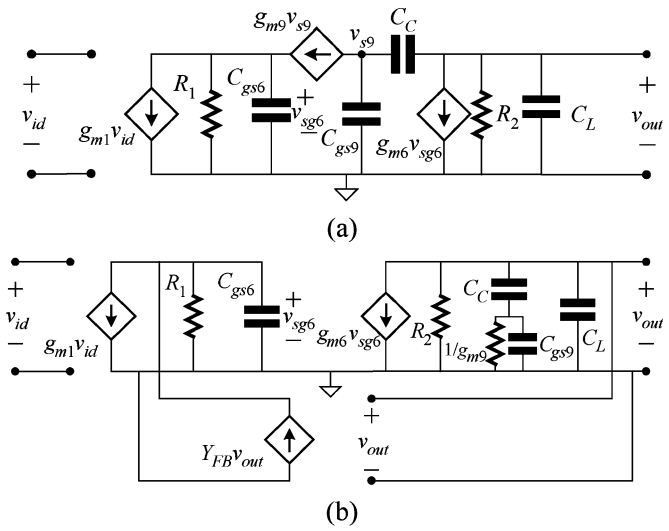

Fig. 3. (a) Small-signal equivalent circuit of the opamp in Fig. 1; (b) equivalent circuit of (a) in classical shunt-shunt feedback configuration.

III. Compensation Strategy

Fig. 3(a) shows the small-signal equivalent circuit of the opamp in Fig. 1. By using direct analysis, the transfer function of the opamp in Fig. 3(a) can be obtained. Alternatively, by using feedback theory, the transfer function can be analyzed from Fig. 3(b) as follows. According to Fig. 3(b), by denoting $Z_{\mathrm{OL}}(s)$ the open-loop transimpedance function and $Y_{FB}(s)$ the transadmittance feedback factor, we obtain

$$A(s) = g_{m1}\frac{Z_{\mathrm{OL}}(s)}{1 + Z_{\mathrm{OL}}(s)Y_{FB}(s)} = \frac{g_{m1}}{Y_{\mathrm{OL}}(s) + Y_{FB}(s)} \tag{8}$$

where under normal condition, $C_{gs8} \ll C_L$ and $R_2 \gg 1/g_{m8}$, we have (9) shown at the bottom of the page and

$$Y_{FB}(s) = \frac{sC_C g_{m9}}{g_{m8} + s(C_C + C_{gs9})} \tag{10}$$

According to (8), we found that the dc gain of the opamp is given by

$$A_o = g_{m1}g_{m6}R_1R_2. \tag{11}$$

Using dominant pole approximation [5], the opamp's dominant pole frequency can be found to be

$$\omega_{p1} \cong \frac{1}{g_{m6}R_1R_2C_C}. \tag{12}$$

By combining (8)–(12), it can also be shown that at $\omega \gg \omega_{p1}$, we have

$$A(s) \cong \frac{\omega_u}{s} \times \frac{1 + s\frac{C_C + C_{gs9}}{g_{m9}}}{s^2\left(\frac{C_L C_{gs6}}{C_C g_{m6}} \times \frac{C_C + C_{gs9}}{g_{m9}}\right) + s\left(\frac{C_L C_{gs6}}{C_C g_{m6}} + \frac{C_{gs6}}{g_{m6}}\right) + 1} \tag{13}$$

$$Y_{\mathrm{OL}}(s) = \frac{(1 + sR_1C_{gs6})\left\{s^2R_2C_L(C_C + C_{gs9}) + s\left[R_2g_{m9}(C_L + C_C)\right] + g_{m9}\right\}}{g_{m6}R_1R_2\left\{g_{m9} + s(C_C + C_{gs9})\right\}} \tag{9}$$

where

$$\omega_u \cong A_o\omega_{p1} = \frac{g_{m1}}{C_C} \tag{14}$$

is the unity-gain frequency, also commonly known as gain-bandwidth product, of the opamp.

By inspecting (13), we found that under the condition

$$\frac{g_{m9}}{C_C + C_{gs9}} = \frac{g_{m6}}{C_{gs6}} \tag{15}$$

the nondominant poles of $A(s)$, i.e., the roots of the polynomial

$$B(s) = s^2\left(\frac{C_L C_{gs6}}{C_C g_{m6}} \times \frac{C_C + C_{gs9}}{g_{m9}}\right) + s\left(\frac{C_L C_{gs6}}{C_C g_{m6}} + \frac{C_{gs6}}{g_{m6}}\right) + 1$$

are real and given by

$$p_2 = -\frac{g_{m6}C_C}{C_{gs6}C_L} \tag{16}$$

$$p_3 = -\frac{g_{m9}}{C_C + C_{gs9}} = -\frac{g_{m6}}{C_{gs6}}. \tag{17}$$

It can be observed that p_3 cancels the finite zero of the transfer function

$$z = -\frac{g_{m9}}{C_C + C_{gs9}} \tag{18}$$

exactly and $A(s)$ can therefore be reduced to

$$A(s) \cong \frac{\omega_u}{s} \times \frac{1}{1 - \frac{s}{p_2}}. \tag{19}$$

According to (19), the phase margin of the opamp, considered for 100% feedback, can be shown to be

$$\phi_M = \tan^{-1}\frac{|p_2|}{\omega_u} = \tan^{-1}\frac{\omega_{T6}C_C}{\omega_u C_L} \tag{20}$$

where by denoting $V_{\text{eff}6} = V_{SG6} - |V_{t6}|$

$$\omega_{T6} = \frac{g_{m6}}{C_{gs6}} = \frac{3}{2}\frac{\mu_p}{L_6^2}V_{\text{eff}6} \tag{21}$$

is the transition frequency of M6. Combining (20) and (21) yields

$$L_6 = \sqrt{\frac{3\mu_p V_{\text{eff}6} C_C}{2\omega_u C_L \tan\phi_M}}. \tag{22}$$

Combining (15), (20), and (21) yields the compensation condition

$$g_{m9} = \tan\phi_M \omega_u C_L\left(1 + \frac{C_{gs9}}{C_C}\right). \tag{23}$$

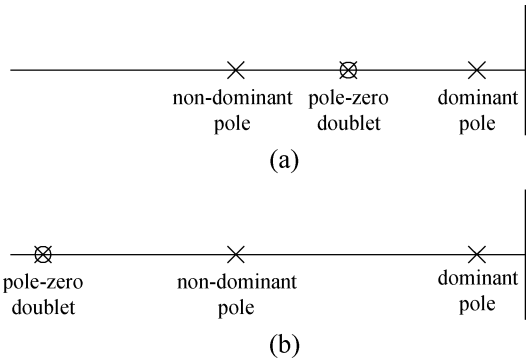

Fig. 4. Location of poles and zeros of the opamps designed by (a) procedure in [3] and (b) proposed procedure.

By substituting the MOS equations

$$g_m = \sqrt{2\mu_n C_{\text{OX}}\left(\frac{W}{L}\right)I_D} \quad \text{and} \quad C_{gs} = \left(\frac{2}{3}\right)WLC_{\text{OX}}$$

into (23) and rearranging the result, we obtain the equation

$$I_{D9} = \frac{(\tan\phi_M\omega_u C_L)^2\left(C_C + \frac{2}{3}W_9L_9C_{\text{OX}}\right)^2}{2\mu_n C_{\text{OX}}\left(\frac{W_9}{L_9}\right)} \tag{24}$$

which can be used in the tradeoff between power consumption and area of the compensation circuit.

Although p_3 and z are designed to cancel out each other, a complete cancellation is difficult to achieve in analog implementation. An incomplete cancellation would result in p_3 and z forming a pole–zero doublet. However, according to (16)–(18), since C_C is generally lower than C_L, the doublet $p_3 - z$ is somewhat higher than p_2. As a result, the proposed strategy would result in the opamp which is more tolerant to the imprecision of the cancellation than the strategy in [3] where the doublet is lower than the nondominant pole, as shown in Fig. 4.

According to (22), it can also be shown that the minimum allowable value of C_C is much smaller and equivalent to those in [2] and [3], respectively. The ability to use smaller C_C provides a higher degree-of-freedom in trading noise performance with power consumption [3].

IV. Design Procedure

Since the dc and transient characteristics of the two-stage CMOS opamp are independent of the compensation method, the design procedure of the opamp in Fig. 1 can obtained by modifying the design procedure in [3], shown here in Table I. The necessary modifications are in Steps 3 and 10 where the compensation conditions of (22) and (24) are applied, i.e.,

Step 3) Use (22) and $V_{\text{eff}6} = V_{\text{HR}}^{out+}$ [3] to compute L_6.

Step 10) Use (24) to choose the values of $(W/L)_9$ and I_{D9}

The proposed design procedure of the opamp in Fig. 1 is shown in Table II.

TABLE I
OPAMP DESIGN PROCEDURES IN [3]

Step 1	$C_C = \frac{16kT}{3\omega_u S_n(f)}\left[1+\frac{SR}{\omega_u(V_{HR}^{CM+}+V_{tn})}\right]$
Step 2	$I_{D7}= SR(C_C + C_L)$
Step 3	$L_6 = \sqrt{\frac{3\mu_p V_{HR}^{out+} C_C}{2\omega_u(C_C + C_L)\tan(\phi_M)}}$
Step 4	$W_6 = \frac{2SR(C_C + C_L)}{\mu_p C_{OX}\left(V_{HR}^{out+}\right)^2} L_6$
Step 5	$I_{D5}= C_C SR$
Step 6	$(W/L)_{1,2} = \frac{\omega_u^2 C_C}{\mu_n C_{OX} SR}$
Step 7	$(W/L)_{5,8} = \frac{2SRC_C}{\mu_n C_{OX}\left(V_{HR}^{CM-} - V_{tn} - SR/\omega_u\right)^2}$
Step 8	$(W/L)_7 = \left(\frac{C_C + C_L}{C_C}\right)(W/L)_{5,8}$
Step 9	$(W/L)_{3,4} = \frac{(W/L)_6}{2(W/L)_7}(W/L)_{5,8}$
Step 10	$(W/L)_9 = \frac{2C_c SR}{\mu_p C_{OX} V_{HR}^{out+}\left(V_{DD} - V_{HR}^{out+} - 2\lvert V_{tp}\rvert\right)}$

TABLE II
PROPOSED OPAMP DESIGN PROCEDURE

Step 1	$C_C = \frac{16kT}{3\omega_u S_n(f)}\left[1+\frac{SR}{\omega_u(V_{HR}^{CM+}+V_{tn})}\right]$
Step 2	$I_{D7}= SR(C_C + C_L)$
Step 3	$L_6 = \sqrt{\frac{3\mu_p V_{HR}^{out+} C_C}{2\omega_u C_L \tan\phi_M}}$
Step 4	$W_6 = \frac{2SR(C_C + C_L)}{\mu_p C_{OX}\left(V_{HR}^{out+}\right)^2} L_6$
Step 5	$I_{D5}= C_C SR$
Step 6	$(W/L)_{1,2} = \frac{\omega_u^2 C_C}{\mu_n C_{OX} SR}$
Step 7	$(W/L)_{5,8} = \frac{2SRC_C}{\mu_n C_{OX}\left(V_{HR}^{CM-} - V_{tn} - SR/\omega_u\right)^2}$
Step 8	$(W/L)_7 = \left(\frac{C_C + C_L}{C_C}\right)(W/L)_{5,8}$
Step 9	$(W/L)_{3,4} = \frac{(W/L)_6}{2(W/L)_7}(W/L)_{5,8}$
Step 10	$I_{D9} = \frac{(\tan\phi_M \omega_u C_L)^2\left(C_C + \frac{2}{3}W_9 L_9 C_{OX}\right)^2}{2\mu_n C_{OX}(W_9/L_9)}$

V. DESIGN EXAMPLE

Fig. 5 shows a two-stage CMOS opamp with robust bias part [7]. For the process parameters shown in Table III and opamp specification shown in Table IV, design parameters of the core circuit and the bias circuit of the opamp in Fig. 5 are obtained from Table II and [7] respectively. These design parameters are shown in Table V and the Synopsis HSPICE V2003.03 simulation results of the designed opamp are shown in Table VI.

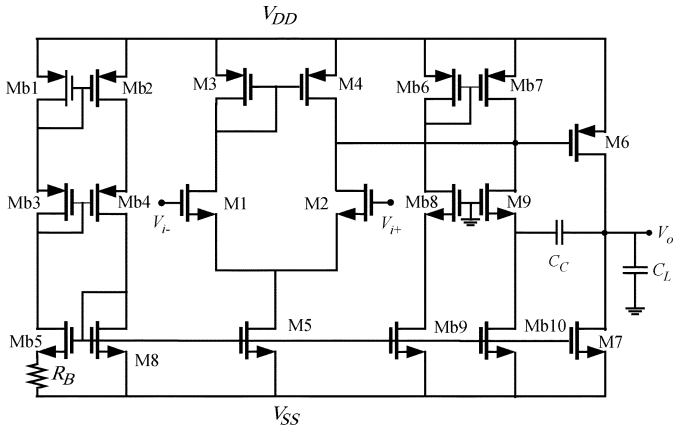

Fig. 5. Opamp with robust bias circuit.

TABLE III
PROCESS PARAMETERS (0.5 MICRON HP'S CMOS14TB)

parameters	NMOS	PMOS
μ [cm^2/Vsec]	506	115.6
V_t [V]	0.7	-0.9
T_{OX} [nm]	9.61	9.61

TABLE IV
OP AMP SPECIFICATION

Supply voltages	±2.5 V
Load capacitance: C_L	5 pF
DC gain: A_o	≥ 80dB
Unity-gain frequency: f_u	5 MHz
Phase margin: ϕ_M	65°
Slew rate: SR	±5.5 V/μsec
Input common-mode range: V_{CMR}	±1.5 V
Output swing: $V_{out(\max,\min)}$	±2.3 V

VI. CONCLUSION

Simulation results confirm that the proposed design procedure can be used to design the opamp that meets all the given specifications. Both the proposed procedure and the strategy proposed in [1] employ the Miller capacitor current buffer compensation. However, while the strategy in [1] results in the opamp with nondominant complex poles, which exhibit peaking in closed-loop frequency response, the proposed design

TABLE V
DESIGN PARAMETERS

$(W/L)_{1,2}$	1.4μm/2μm
$(W/L)_{3,4}$	1.8 μm /1 μm
$(W/L)_{5,8}$	1.6 μm /1 μm
$(W/L)_{6}$	85 μm /2.2 μm
$(W/L)_{7}$	17 μm /1 μm
$(W/L)_{9}$	27 μm /1 μm
$(W/L)_{b1\text{-}b4}$	1.6 μm /1 μm
$(W/L)_{b5}$	6.4 μm /1 μm
$(W/L)_{b6\text{-}b7}$	131 μm /1 μm
$(W/L)_{b8}$	27 μm /1 μm
$(W/L)_{b9\text{-}b10}$	7.4 μm /1 μm
R_B	32 kΩ
C_C	0.5 pF

TABLE VI
SIMULATED RESULTS

A_o	81 dB
f_u	5 MHz
ϕ_M	65°
$SR+$	6.5 V/μsec
$SR-$	-5.9 V/μsec
V_{CMR+}	2.15 V
V_{CMR-}	-1.98 V
$V_{out(\max)}$	2.3 V
$V_{out(\min)}$	-2.4 V
Input offset voltage	318 μV
Input noise at 10KHz	157 nV/$\sqrt{\text{Hz}}$
Power dissipation	378 μW

procedure results in the opamp with only one nondominant real pole, which exhibits flat closed-loop frequency response. Comparison between the proposed procedure and the other procedures are summarized below.

- Compared to the procedure based upon the nullifying resistor compensation in [2]: The value of C_C of the proposed procedure can be made much smaller than in [2]. The wider range of the allowable value of C_C provides a higher flexibility for noise-power tradeoff [3].
- Compared to the procedure in [3]: Both procedures rely on pole–zero cancellation. However, as shown in Fig. 4, the proposed procedure is less sensitive to the exactness of the cancellation because the pole–zero doublet is placed much higher than the nondominant pole.

ACKNOWLEDGMENT

The author gratefully acknowledges the contribution of P. Durongdumrongchai to this work.

REFERENCES

[1] G. Palmisano and G. Paumbo, "A compensation strategy for two-stage CMOS opamps based on current buffer," *IEEE Trans. Circuits Syst. I, Fundam. Theory Appl.*, vol. 44, no. 3, pp. 257–262, Mar. 1997.

[2] G. Palmisano, G. Palumbo, and S. Pennisi, "Design procedure for two-stage CMOS transconductance amplifier: a tutorial," in *Analog Integrated Circuit and Signal Processing*. Norwell, MA: Kluwer, 2001, vol. 27, pp. 179–189.

[3] J. Mahattanakul and J. Chutichatuporn, "Design procedure for two-stage CMOS opamp with flexible noise-power balancing scheme," *IEEE Trans. Circuits Syst. I, Fundam. Theory Appl.*, vol. 52, no. 8, pp. 1508–1514, Aug. 2005.

[4] B. K. Ahuja, "An improved frequency compensation technique for CMOS operational amplifiers," *IEEE J. Solid-State Circuits*, vol. SC-18, no. 3, pp. 629–633, Jun. 1983.

[5] P. E. Allen and D. R. Holberg, *CMOS Analog Circuit Design*, 2nd ed. Oxford, U.K.: Oxford, 2002.

[6] P. R. Gray, P. J. Hurst, S. H. Lewis, and R. G. Meyer, *Analysis and Design of Analog Integrated Circuits*, 4th ed. New York: Wiley, 2001.

[7] D. A. Johns and K. Martin, *Analog Integrated Circuit Design*. New York: Wiley, 1997.